

# Numerical and Experimental Study of Buckling of Rectangular Steel Plates with a Cutout

M. Shariati<sup>1,\*</sup>, Y. Faradjian<sup>2</sup>, H. Mehrabi<sup>2</sup>

<sup>1</sup>Department of Mechanical Engineering, Ferdowsi University of Mashhad, Mashhad, Iran

<sup>2</sup>Department of Mechanical Engineering, Shahrood University of Technology, Shahrood, Iran

Received 8 November 2015; accepted 7 January 2016

## ABSTRACT

Steel plates are used in various structures, such as the structures of the deck and body of ships, bridges, and aerospace industry. In this study, we investigate the buckling and post-buckling behavior of rectangular steel plates having circular cutouts with two boundary conditions: first, clamped supports at upper and lower ends and free supports at other edges; second, clamped supports at upper and lower ends and simply supports at other edges, using finite element method (by ABAQUS software) and experimental tests (by an INSTRON servo hydraulic machine). In this research, in addition to the aspect ratio, the effect of changing the location of the cutout on the buckling analysis is investigated. The results of both numerical and experimental analyses are compared and showing a very good agreement between them.

© 2016 IAU, Arak Branch. All rights reserved.

**Keywords :** Buckling; Steel plates; Cutout; Experimental analysis; FEM.

## 1 INTRODUCTION

THE problem of the buckling of rectangular plates with simply supports in four edges, with length, width, and thickness, was first considered by Timoshenko in 1961 [1]. Khaled et al. used the FEM method to determine the buckling load of the plates [2]. They assumed simply boundary conditions for all four edges and investigated aspect ratios of 1 to 4 to determine the effect of this parameter on the buckling load. They studied two cutout geometries, including circular cutouts and rectangular cutouts with rounded corners, with cutout center situated in different points of the plate. Furthermore, Khaled used the FEM method for determination of the buckling load of plates with circular cutouts [3]. They assumed linear elastic and complete plastic characteristics for the material and ignored the stiffness issue. Narayanan studied the ultimate strength of plates with cutouts under axial compression loads [4]. He used an approximate method for determining the buckling load and confirmed his theoretical work with empirical results. In that study, he used square plates with circular and square-shaped cutouts and investigated the effect of cutout diameter and plate thickness on the buckling behavior. Shanmagan studied the buckling and post-buckling behavior of plates with cutout and various boundary conditions under uniaxial and biaxial compression loading [5]. He used the finite element analysis software ABAQUS for investigating the buckling behavior of square-shaped plates with circular and rectangular cutouts. He studied various parameters, including cutout shape and size, plate thickness, boundary conditions, and the type of loading. Roberts also used the FEM method for investigation of the elasto-plastic buckling of plates with cutouts [6]. Furthermore, Mingot proposed that for investigation of the buckling of plates with cutout. They proposed that this problem can be reduced to the buckling of plates without cutouts using a method called homogenization [7]. Brown studied the stability of square plates using the direct

\*Corresponding author. Tel.: +98 9121733750.

E-mail address: mshariati44@um.ac.ir (M. Shariati).

matrix method [8]. Maan used the fixed grid finite element analysis (FGFEA) method to solve the buckling problem [9]. Anada studied the buckling eigenvalue for double joint plates [10]. He used square and rectangular plates with central cutouts. He calculated a buckling coefficient for above-mentioned plates and compared his results with the existing findings and the finite element analysis results.

The elastic buckling behavior of rectangular perforated plates was studied using the finite element method by Komur et al. [11]. They chosen circular cutout at different locations along the principal x-axis of plates subjected to linearly varying loading in order to evaluate the effect of cutout location on the buckling behavior of plates. Their results show that the center of a circular hole should not be placed at the end half of the outer panel for all loading patterns. Furthermore, the presence of a circular hole always causes a decrease in the elastic buckling load of plates. A new approximate procedure for buckling analysis of simply supported rectangular stepped or perforated plates subjected to uniform edge stresses is formulated by Rahai et al. [12]. The procedure uses energy method based on modified buckling mode shapes. Eccher et al. [13] provided the application of the isoparametric spline finite strip method to the elastic buckling analysis of perforated folded plate structures. The general theory of the isoparametric spline finite strip method is introduced. The linear buckling analyses of square and rectangular plates with circular and rectangular holes in various positions subjected to axial compression and bending moment are developed has been studied by Maiorana et al. [14]. The aim of their paper is to give some practical indications on the best position of the circular hole and the best position and orientation of rectangular holes in steel plates, when axial compression and bending moment act together. Eccher G, et al. [15] introduced the general theory of the isoparametric spline finite strip method for buckling of perforated plates. The reliability of their method is demonstrated by applying the method to classical nonlinear complex plate and shell problems as well as the geometric nonlinear analysis of perforated flat and stiffened plates. Also, Jeom Kee Paik[16] has been studied ultimate strength of perforated steel plates under axial compressive loading along short edges using Finite Element Method. The plates are considered to be simply supported along all (four) edges, keeping them straight. The cutout is circular and located at the center of the plate.

In this study, we investigate the buckling and post-buckling behavior of steel rectangular plates having circular cutouts with two boundary conditions: first, clamped supports at upper and lower ends and free supports at other edges; second, clamped supports at upper and lower ends and simply supports at other edges, using numerical analysis and experimental methods. The locations of cutouts are interchanged vertically and horizontally on the plates. The results of both numerical and experimental analyses are compared and showing a very good agreement between them.

## 2 MECHANICAL PROPERTIES OF THE PLATES

In order to determine the mechanical characteristics of the specimens, a tensile test was performed according to the ASTM-E8 standard using a servo hydraulic INSTRON machine, and the Young modulus, yield stress, and plastic properties were determined. The stress-strain curve is plotted using the data derived from standard tensile test as shown in Fig. 1. The real stress-strain curve characteristics are also required for non-linear analysis with the finite element ABAQUS software. The real stress and strain are computed using the following relationship.

$$\epsilon_{pl} = \epsilon_{real} - \frac{\sigma_{real}}{E} \tag{1}$$

$$\epsilon_{real} = \ln(1 + \epsilon_{Eng.}) \tag{2}$$

$$\sigma_{real} = \sigma_{Eng.} (1 + \epsilon_{Eng.}) \tag{3}$$

Based on the linear section of the real stress-strain curve, the Young modulus was calculated as E=217 GPa and the yield stress was computed as  $\sigma_y=350$  MPa . Furthermore, the value for the Poisson ratio was assumed to be  $\nu=0.33$ .

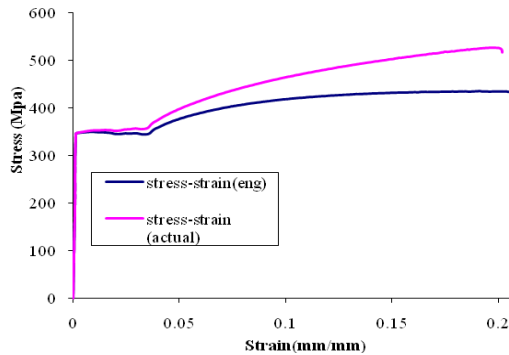


**Fig.1**  
Experimental stress-strain curve for used steel.

### 3 GEOMETRY OF THE SPECIMENS

In this study, we used plates with width of 100 mm, lengths of 110, 150, 160 and 210 mm, and thickness of 2.07 mm. The cutouts were circular cutout with a 10 mm radius. A schematic view of a specimen with a circular cutout is shown in Fig. 2, where  $a$  and  $b$  are length and width of plate respectively,  $c$  and  $d$  are distances of cutout center from centerlines of plate and  $e$  is radius of the cutout.

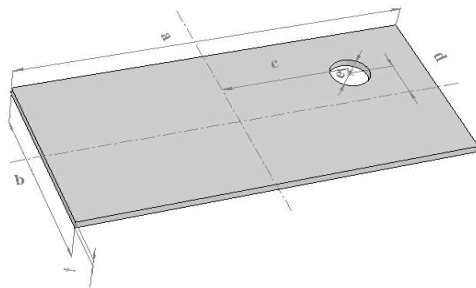


**Fig.2**  
Geometry of plate with circular cutout.

### 4 BOUNDARY CONDITIONS

In the numerical analysis, for the first boundary condition we modeled two solid planes attached to upper and lower ends of the plates for application of the boundary conditions on the edges of the rectangular plates. The load was applied in concentric form upon the center of the upper solid plane, and resulted in an extensive compression loading on both clamped edges of the plate. All degrees of freedom of the lower plane, as well as all degrees of freedom of the upper plane, except for movement in the direction of the axis (the longitudinal direction of the plate) were constrained. Accordingly, the boundary conditions were free for the side edges (vertical edges) and clamped for the upper and lower edges, which is represented as CFCF (Clamped-Free-Clamped-Free). For second boundary condition the free edges were constrained in the form of simply supported.

### 5 MESH GENERATION OF THE SPECIMENS

For meshing of the specimens, we have used the non-linear element S8R, a quadratic element consisting of 8 nodes with 6 degrees of freedom, which is suitable for relatively thin walled shells. This element has appropriate degrees of freedom for modeling the specimens and the boundary conditions. In the element S8R, the shear stress is also taken into account, and this increases the precision of the results. In this element, a reduced integral is used for calculation of the stiffness matrix. However, mass and load matrices are integrated using the exact method. Reduced integral usually produces more accurate results, provided that the elements are not damaged and are not subjected to

in-plane bending loads. Additionally, this method reduces the computation time. Evaluation of the results and comparison with the experimental results show that the chosen element has been appropriate for this study. In specimens with cutouts, elements have been made smaller in proximity to the cutouts in order to enhance the precision of the computations. The mesh generation configuration around the cutout is shown in Fig. 3.

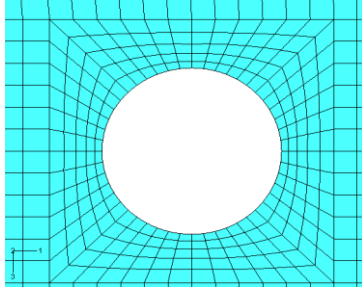


**Fig.3**  
Mesh generation around of circular cutout.

**6 NUMERICAL PROCEDURE**

As it has been pointed out previously, linear analysis, especially for thin plates, overestimates the buckling load related to the actual value. Nevertheless, an (eigenvalue) linear analysis is initially performed for all specimens to obtain the shape of modes that have lower eigenvalues, since the buckling usually occurs in the first mode shape. The displacements for these modes are saved in a file and used in the next analysis (Static, Riks), so that the effect of mode shapes are taken into account in the buckling analysis.

For non-linear analysis, the mode shape of the actual buckling of the plate (which has been the first mode shape for the present experimental analysis) and the initial imperfection should be supplied to the software. For this purpose, the value of the initial imperfection of the specimens was measured in laboratory for all specimens before the numerical analysis. After completion of this step, we observed that the average initial imperfection is about 25% of the plate thickness. However, for higher precision, we measured experimentally the initial imperfection of each specimen separately and used the obtained values as inputs for the numerical analysis software.

**7 RESULTS OF FINITE ELEMENT ANALYSIS FOR THE FIRST BOUNDARY CONDITION**

Figs. 4-7 show the load-displacement curves resulting from the numerical analysis performed with ABAQUS software for specimens with one circular cutout with aspect ratios of 1:1, 1:6, and 2:1. Load-displacement curve of specimens with one circular cutout with an aspect ratio of 1:5 is shown in Fig. 7. Fig. 8 shows the buckling mode of the specimen pl-150-100, 07-49, 97-0-20, 2-2, 05 after nonlinear analysis accompanied by Von Mises stress contour. For the sake of comparison, Table 1. shows the buckling loads and the initial imperfections of specimens with aspect ratios of 1:1, 1:6, and 2:1. Also, the buckling loads and the initial imperfections for specimens with aspect ratio of 1:5 are shown in Table 2.

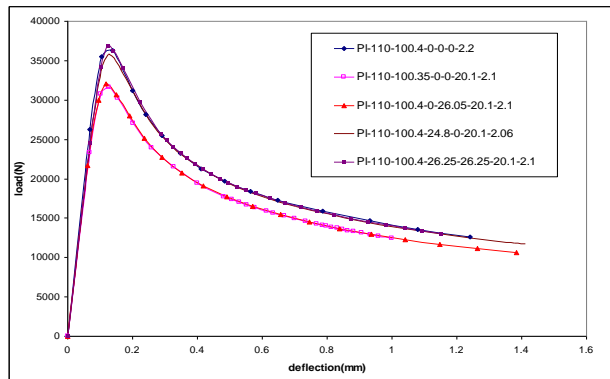


**Fig.4**  
Load-displacement curve for specimens with aspect ratio 1.1.

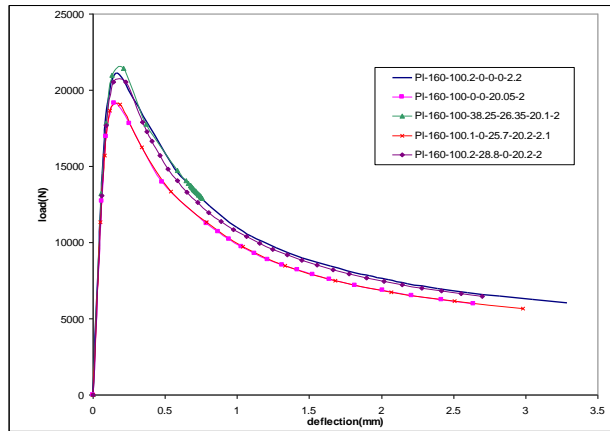


**Fig.5**  
Load-displacement curve for specimens with aspect ratio 1.6.

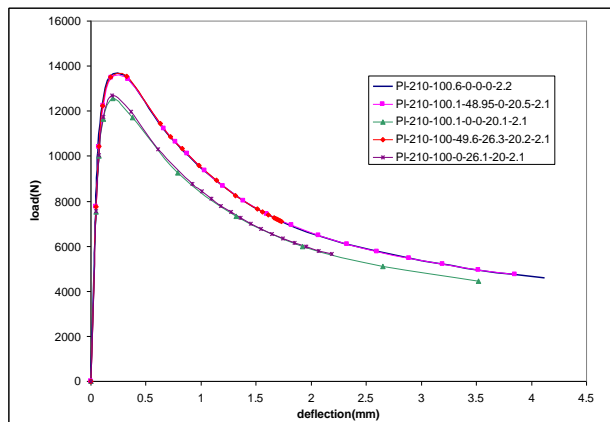


**Fig.6**  
Load-displacement curve for specimens with aspect ratio 2.1.

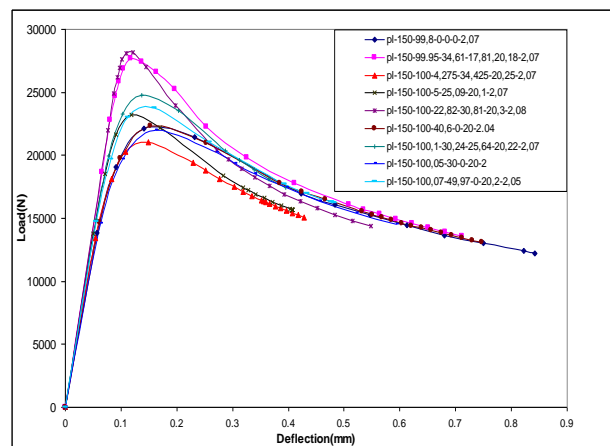


**Fig.7**  
Load-displacement curve for specimens with aspect ratio 1.5.

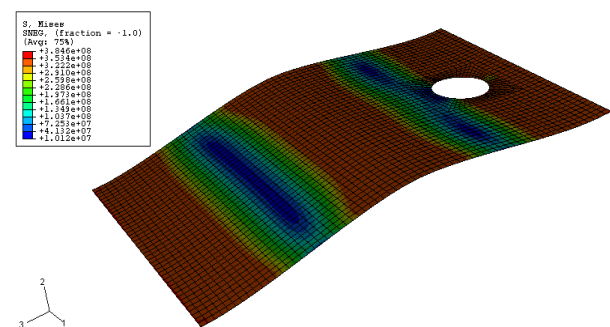


**Fig.8**  
Buckling mode shape of pl-150-100,07-49,97-0-20,2-2,05 specimen.

**Table 1**  
Finite element results of specimens with a circular cutout with aspect ratios of 1.1, 1.6 and 2.1.

Specimen name	Aspect ratio	Imperfection (m)	P <sub>cr</sub> (N)
pl-110-100.4-0-0-0-2.2	1.1	0.00044	36286.6
pl-110-100.35-0-0-20.1-2.1	1.1	0.00042	31599.6
pl-110-100.4-0-26.05-20.1-2.1	1.1	0.00042	32064.4
pl-110-100.4-24.8-0-20.1-2.06	1.1	0.000412	35784.5
pl-110-100.4-26.25-26.25-20.1-2.1	1.1	0.00042	36864.1
pl-160-100.2-0-0-0-2.2	1.6	0.00055	21829.8
pl-160-100-0-0-20.05-2	1.6	0.0005	19167.5
pl-160-100-38.25-26.35-20.1-2	1.6	0.000325	21425.5
pl-160-100.1-0-25.7-20.2-2.1	1.6	0.000525	19079.9
pl-160-100.2-28.8-0-20.2-2	1.6	0.0005	20550.3
pl-210-100-0-26.1-20-2.1	2.1	0.000525	12692.6
pl-210-100-49.6-26.3-20.2-2.1	2.1	0.000525	13532.7
pl-210-100.1-0-0-20.1-2.1	2.1	0.000525	12576
pl-210-100.1-48.95-0-20.5-2.1	2.1	0.000525	12480.4
pl-210-100.6-0-0-0-2.2	2.1	0.00055	13546.3

**Table 2**  
Finite element results of specimens with a circular cutout with aspect ratios of 1.5.

Specimen name	Imperfection (m)	P <sub>cr</sub> (N)
pl-150-99,8-0-0-0-2,07	0.00058	22112.8
pl-150-99,95-34,61-17,81-20,18-2,07	0.0001	27679.8
pl-150-100-4,275-34,425-20,25-2,07	0.00045	21044.3
pl-150-100-5-25,09-20,1-2,07	0.00025	23234.2
pl-150-100-22,82-30,81-20,3-2,08	0.00005	28171.3
pl-150-100-40,6-0-20-2,04	0.00055	22340
pl-150-100,1-30,24-25,64-20,22-2,07	0.0003	24799.6
pl-150-100,05-30-0-20-2	0.00058	21981.3
pl-150-100,07-49,97-0-20,2-2,05	0.00035	23778.5

It is evident that as aspect ratio increases, the buckling load decreases considerably. For example, in specimens without any cutouts, increasing the aspect ratio from 1:1 to 2:1, leads to 62% decrease in the buckling load. The findings of this study showed that, as expected, with equal initial imperfections, the specimen without holes has the highest buckling load.

In the specimen pl-110-100.4-0-0-0-2.2, due to greater initial imperfection, the buckling load is about 600 N lower than the specimen pl-110-100.4-26.25-26.25-20.1-2.1. But for two aspect ratios of 1:6 and 2:1, the specimen without cutouts has the highest buckling load.

Another important result is that displacement of the cutout from the center of the plate in the transverse direction has little effect on decreasing the buckling load. Provided that no longitudinal displacement occurs, displacement of the cutout in the transverse direction causes about 2% change in the buckling load in specimens with cutouts with aspect ratios of 1:1, 1:6, and 2:1. Investigations showed that when longitudinal displacement of the cutout from the center of the plate exceeds a certain limit, it has little more effect on decreasing the buckling load. For example, in the specimen pl-160-100-38.25-26.35-20.1-2, where the distance from the center of the cutout to the center of the plate is 38.25 mm in the longitudinal direction, the difference in the buckling load with the specimen without cutouts is less than 2%. While the difference of the buckling load between the specimen pl-160-100.1-0-25.7-20.2-2.1 and the specimen without cutouts with the same aspect ratio is 12%, because the cutout lies in the effective longitudinal distance from the center of the plate. Additionally, the results show that the presence of this cutout with a diameter of 0.2 b does not decrease the buckling load more than 12% in specimens with aspect ratios of 1:1, 1:6, and 2:1.

In specimens with aspect ratio of 1:5, the large effect of the initial imperfection is clearly seen, so that the specimens pl-150-100-22, 82-30, 81-20, 3-2, 08 and pl-150-99.95-34, 61-17, 81, 20, 18-2, 07, with smaller initial imperfections in comparison with the other specimens, have the highest buckling loads, and the buckling load of the specimen without cutouts is considerably lower than these specimens due to the large initial imperfection. With identical initial imperfections, the specimen without cutouts is comparable to the specimen pl-150-100, 05-30-0-20-2, where the existence of the cutout has reduced the buckling load by only 0.6%. It can be easily deduced that this cutout is situated outside the longitudinal effective domain around the center of the plate. In the specimens pl-150-100, 05-30-0-20-2 and pl-150-100-40, 6-0-20-2.04, where the initial imperfections are approximately similar, the

loads are seen to be almost identical, while the longitudinal distance of the center of the circular cutout has increased by about 10 mm. Accordingly, we can conclude that when the cutout is outside the effective longitudinal distance from the middle of the plate, displacement of the cutout has little effect on the buckling load. Furthermore, the smallest buckling load for this aspect ratio belongs to the specimen pl-150-100-4, 275-34, 425-20, 25-2, 07, because not only the cutout lies in the effective domain, but also there is a relatively large initial imperfection in this specimen.

## 8 MEASUREMENT OF THE INITIAL IMPERFECTION

As stated previously, due to the importance of the amount of initial imperfection on the buckling load, the value of the initial imperfection for all specimens must be measured experimentally prior to testing for buckling. This parameter was measured using an INSTRON servo hydraulic machine test under load control with acceptable accuracy as shown in Fig.9. For this purpose, the amount of the initial curvature of plates is obtained by pressing the specimen along its thickness using actuator of machine test and drawing of its load-displacement diagram simultaneously.



**Fig.9**

The procedure that is used for measuring of the initial curvature of plates by an experimental test: (a) Before pressing the plate by force  $F$  ( $\delta$  is initial imperfection), (b) After pressing the plate by force  $F$ .

The value of initial imperfection can be easily calculated by plotting the load- displacement curve. As an example, the load-displacement curve produced for the specimen pl-160-100-38.25-26.35-20.1-2 is shown in Fig. 10. As can be easily observed, the amount of initial imperfection in this specimen is 0.325 mm, because the magnitude of force has increased with a steep slope without any increase in the displacement.

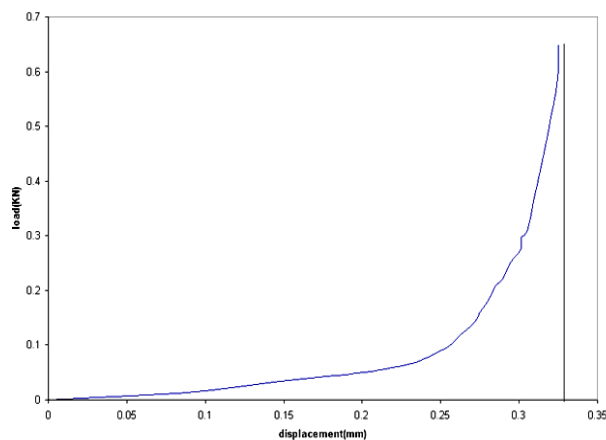


**Fig.10**

Determination of initial imperfection due to curve obtained from experimental test for pl-160-100-38.25-26.35-20.1-2.

## 9 THE EXPERIMENTAL BUCKLING TESTS FOR THE FIRST BOUNDARY CONDITION

For experimental testing of the buckling of rectangular plates, were used from a INSTRON servo hydraulic machine under displacement control. The hydraulic grips of the machine hold the upper and lower edges of the specimens with clamped boundary condition. Also, the lateral edges were free. Therefore, a CFCF boundary condition is created for the plate (as shown in Fig. 11).



**Fig.11**  
Plates in hydraulic clamped grips.

**10 RESULTS OF THE EXPERIMENTAL TESTS**

Similar to the results of numerical analysis, the results of the experimental analysis are classified into multiple categories and are presented accordingly. For each group of the specimens, we present figures related to the buckling mode of the specimens, load-displacement curves, and a table summarizing the buckling load and the initial imperfection.

Figs. 12-14 show the load-displacement curves resulting from experimental analysis for specimens with circular cutout and aspect ratios of 1:1, 1:6, and 2:1. Load-displacement curve of the experimental analysis of specimens with an aspect ratio of 1:5 is shown in Fig. 15. Fig. 16 shows the buckling mode of the specimens pl-210-100-49.6-26.3-20.2-2.1 and pl-150-100.07-49.97-0-20.2-2.1.

To facilitate comparison, Table 3. shows the buckling loads of experimental analysis and the initial imperfections for specimens with circular cutout and aspect ratios of 1:1, 1:6, and 2:1. The experimental buckling load and the initial imperfection for specimens with aspect ratio of 1:5 are shown in Table 3.

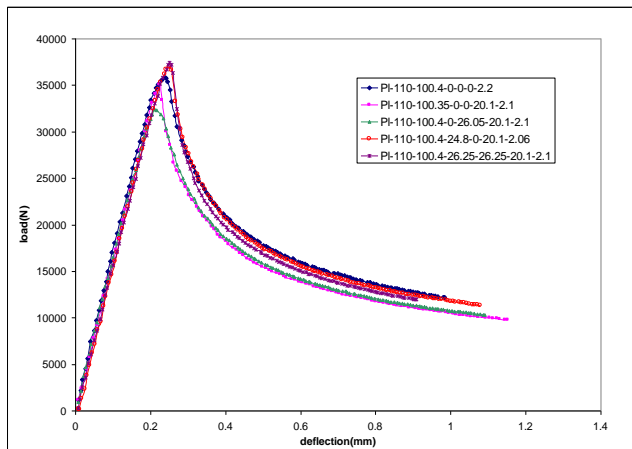


**Fig.12**  
Load-displacement curve of specimen with aspect ratio of 1.1.

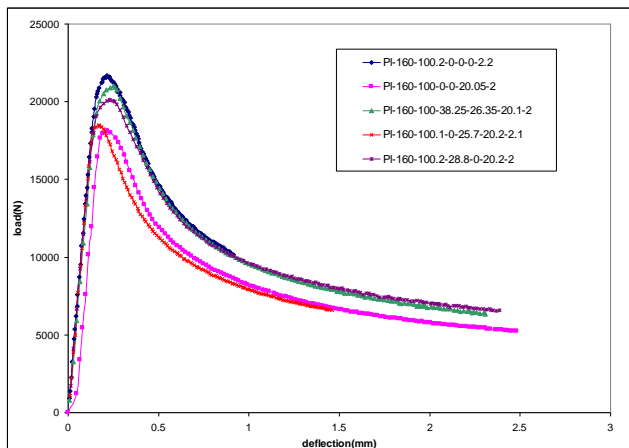


**Fig.13**  
Load-displacement curve of specimen with aspect ratio of 1.6.

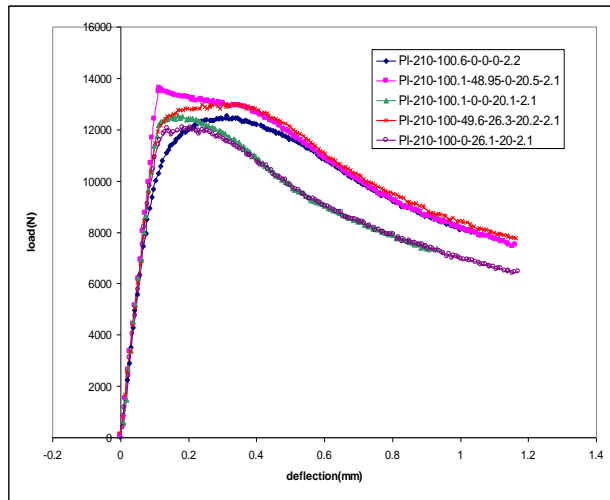


**Fig.14**  
Load-displacement curve of specimen with aspect ratio of 2.1.

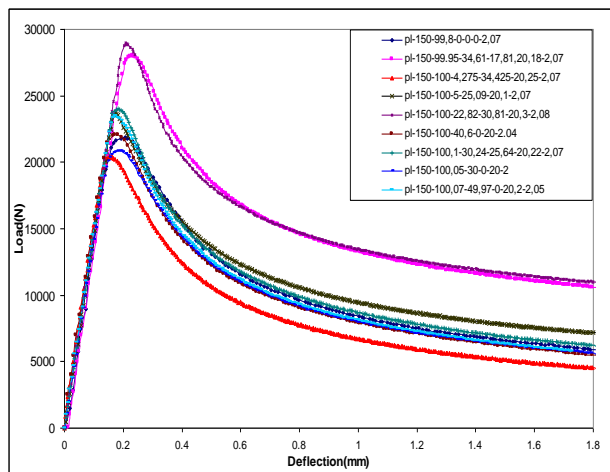


**Fig.15**  
Load-displacement curve of specimen with aspect ratio of 1.5.



**Fig.16**  
Specimens with circular cutouts under experimental buckling tests: (a) pl-150-100.07-49.97-0-20.2-2.1 specimen. (b) pl-210-100-49.6-26.3-20.2-2.1 specimen.

**Table 3**

Experimental results for specimens with circular cutouts with aspect ratios 1.1, 1.6 and 2.1.

Specimen name	Aspect ratio	Imperfection (m)	$P_{cr}$ (N)
pl-110-100.4-0-0-0-2.2	1.1	0.00044	35819.1
pl-110-100.35-0-0-20.1-2.1	1.1	0.00042	35188
pl-110-100.4-0-26.05-20.1-2.1	1.1	0.00042	32335.6
pl-110-100.4-24.8-0-20.1-2.06	1.1	0.000412	36643
pl-110-100.4-26.25-26.25-20.1-2.1	1.1	0.00042	37184.8
pl-160-100.2-0-0-0-2.2	1.6	0.00055	21594.5
pl-160-100-0-0-20.05-2	1.6	0.0005	18109.6
pl-160-100-38.25-26.35-20.1-2	1.6	0.000325	20938.3
pl-160-100.1-0-25.7-20.2-2.1	1.6	0.000525	18406.1
pl-160-100.2-28.8-0-20.2-2	1.6	0.0005	20099.6
pl-210-100-0-26.1-20-2.1	2.1	0.000525	12092.5
pl-210-100-49.6-26.3-20.2-2.1	2.1	0.000525	12963.3
pl-210-100.1-0-0-20.1-2.1	2.1	0.000525	12546.4
pl-210-100.1-48.95-0-20.5-2.1	2.1	0.000525	13475.1
pl-210-100.6-0-0-0-2.2	2.1	0.00055	12537.5

**Table 4**

Experimental results for specimens with circular cutouts with aspect ratios 1.5.

Specimen name	Imperfection (m)	$P_{cr}$ (N)
pl-150-99,8-0-0-0-2,07	0.00058	21882.24
pl-150-99,95-34,61-17,81-20,18-2,07	0.0001	28044.2
pl-150-100-4,275-34,425-20,25-2,07	0.00045	20408.9
pl-150-100-5-25,09-20,1-2,07	0.00025	23734.8
pl-150-100-22,82-30,81-20,3-2,08	0.00005	28964.8
pl-150-100-40,6-0-20-2,04	0.00055	22063.6
pl-150-100,1-30,24-25,64-20,22-2,07	0.0003	24051.24
pl-150-100,05-30-0-20-2	0.00058	20869.6
pl-150-100,07-49,97-0-20,2-2,05	0.00035	23503.74

The experimental analysis, similar to the numerical analysis, evidently shows that with increasing the aspect ratio, the buckling load of the specimens considerably decreases. For example, in specimens without any cutouts, increasing the aspect ratio from 1:1 to 2:1, leads to 64% decrease in the buckling load.

The results of this study showed that, as expected, with equal initial imperfections, the specimen without cutouts has the highest buckling load. For specimens with aspect ratios of 1:1 and 1:2, the maximum buckling load is not observed for the specimen without cutouts due to its higher amount of initial imperfection, but is observed in a specimen in which the hole has been moved in the longitudinal direction away from the middle of the plate.

Also in experimental results, it can be observed that when the cutout is more than 20% away from the middle of the plate in the longitudinal direction, it has little effect on decreasing the buckling load. Displacement of the cutout in transverse direction by the amount specified in this study had little effect on the buckling load.

As an example, in the specimen pl-160-100-38.25-26.35-20.1-2, where the distance between the center of the cutout and the middle of the plate is 38.25 mm in the longitudinal direction, the buckling load is less than 3% different from the specimen without cutouts. On the other hand, the buckling load of the specimen pl-160-100.1-0-25.7-20.2-2.1 has a difference of 14% with the specimen without cutouts, because the cutout lies in the effective longitudinal distance from the center of the plate.

In specimens with aspect ratio of 1:5, the importance of the initial imperfection is clearly seen, so that the specimens pl-150-100-22, 82-30, 81-20, 3-2, 08 and pl-150-99.95-34, 61-17, 81, 20, 18-2, 07, which have relatively smaller initial imperfections compared to the other specimens, have the highest buckling loads, and the buckling load of the specimen without cutouts is much lower than these specimens due to the high degree of initial imperfection. In specimens with identical initial imperfections, the specimen without cutouts is comparable to the specimen pl-150-100, 05-30-0-20-2, where the existence of the cutout has decreased the buckling load by about 4%. Furthermore, it is noticed that if the cutout is not situated in the effective distance from the center of the plate in the longitudinal direction, displacement of the cutout outside this domain, will have little effect on the buckling load. For this aspect ratio, the lowest buckling load pertains to the specimen pl-150-100-4, 275-34, 425-20, 25-2, 07, because the cutout is in the effective longitudinal distance from the center of the plate and there is a relatively large initial imperfection.

## 11 COMPARISON OF THE RESULTS

Figs. 17-21 show the load-displacement curves produced by finite element analysis and the results of experimental tests on some of the specimens. In Fig. 21, the experimental buckling mode of some specimens is compared to the buckling mode calculated by numerical analysis performed with ABAQUS software.

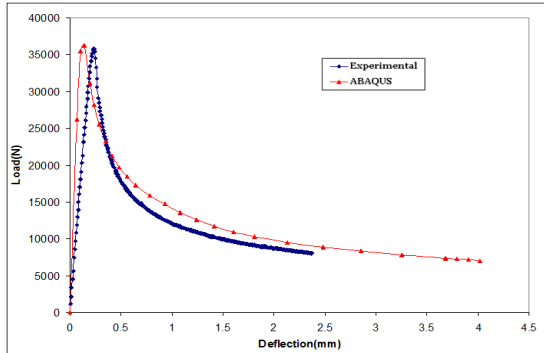


**Fig.17**  
Load-displacement curve of specimen pl-110-100.4-0-0-0-2.2.

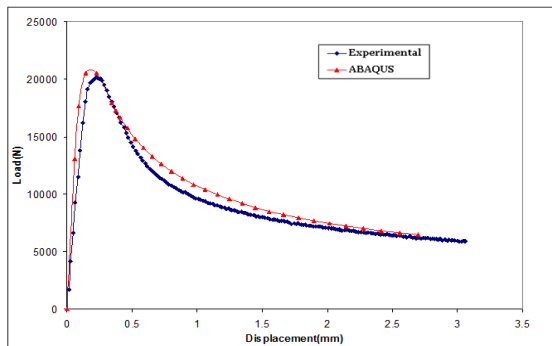


**Fig.18**  
Load-displacement curve of specimen pl-160-100.2-28.8-0-20.2-2.

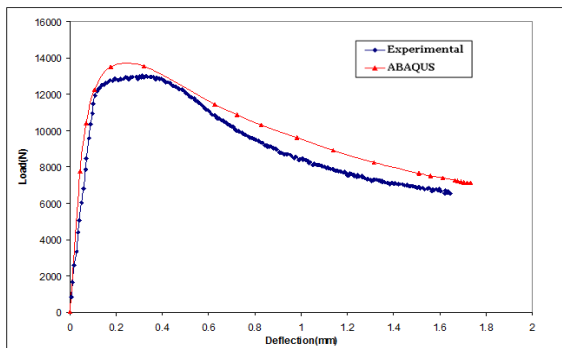


**Fig.19**  
Load-displacement curve of specimen pl-210-100-49.6-26.3-20.2-2.1.

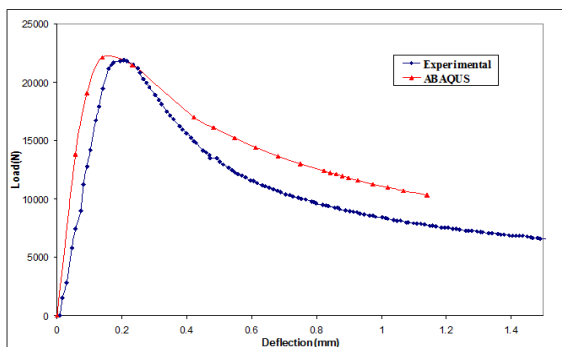


**Fig.20**  
Load-displacement curve of specimen pl-150-99, 8-0-0-0-2,07.

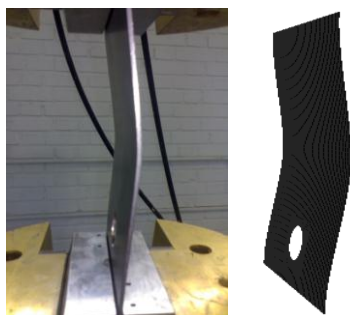


**Fig.21**  
Experimental and numerical buckling mode shapes of specimen pl-150-100,07-49,97-0-20,2-2,05.

## 12 EFFECTS OF BOUNDARY CONDITION

In order to investigate the effects of boundary condition on buckling and post-buckling behavior of steel plates, the second boundary condition was considered. For this aim, the steel plates were considered with clamped support at upper and lower ends and simply supported at other edges. Since providing this boundary condition is not possible with the current equipment of the INSTRON 8802 servo hydraulic machine and the accuracy of the numerical results were quite satisfactory for the first boundary condition, the second boundary condition were investigated numerically with ABAQUS software. It is worth mentioning that providing the appropriate condition to perform such tests could be possible with designing a special fixture which will be considered for our future works. The specimen names and their buckling loads are listed in Table 5.

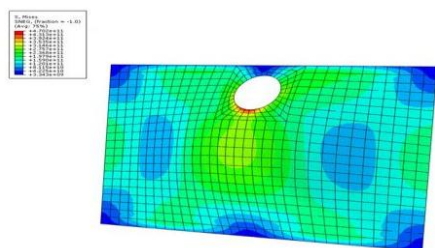
**Table5**

FEM results for specimens with a circular cutout and second boundary condition.

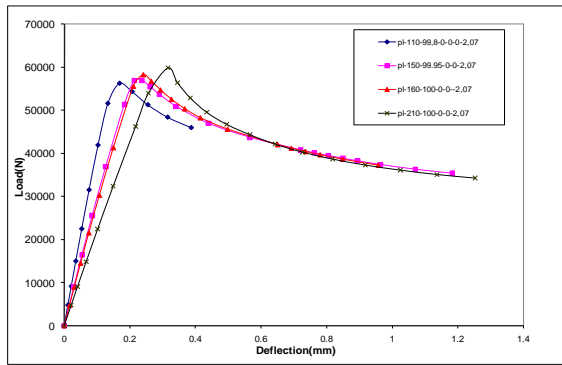
Specimen name	Imperfection (m)	$P_{cr}$ (N)
pl-110-99,8-0-0-0-2,07	0.00044	56231.2
pl-160-99,8-0-0-0-2,07	0.00055	58297.3
pl-210-99,8-0-0-0-2,07	0.00055	59788.5
pl-150-99,8-0-0-0-2,07	0.00058	56889.9
pl-150-99,95-34,61-17,81-20,18-2,07	0.0001	53521.9
pl-150-100-4,275-34,425-20,25-2,07	0.00045	46084.6
pl-150-100-5-25,09-20,1-2,07	0.00025	48583.5
pl-150-100-22,82-30,81-20,3-2,08	0.00005	49891.5
pl-150-100-40,6-0-20-2,04	0.00055	55589.1
pl-150-100,1-30,24-25,64-20,22-2,07	0.0003	50853.1
pl-150-100,05-30-0-20-2	0.00058	52210.4
pl-150-100,07-49,97-0-20,2-2,05	0.00035	56904.7

Fig. 22 shows the mode shape of specimen pl-150-100-4, 275-34, 425-20, 25-2, 07 which is simulated in ABAQUS software. As can be seen, all edges are considered constrained.

Fig. 23 shows the buckling behavior of the steel plates with no cutout and different aspect ratios with clamped support at upper and lower ends and simply supported at other edges. It can be seen that the values of buckling loads were increased significantly in comparison to the first boundary condition. Moreover, as the aspect ratio increases, the buckling load increases. This behavior is different from that observed for the first boundary condition. Therefore, it can be concluded that the boundary condition could have a significant effect on buckling behavior of the steel plates.



**Fig.22**  
Buckling mode shape of pl-150-100-4, 275-34, 425-20, 25-2, 07 specimen.



**Fig.23**  
Load-displacement curve of specimens with different aspect ratio and without cutout.

Fig. 24 shows the buckling behavior of the specimens with aspect ratios of 1.5 and a circular cutout. With the current boundary condition the effect of initial imperfection is not significant. The specimens pl-150-100-22, 82-30, 81-20, 3-2, 08 and pl-150-99.95-34, 61-17, 81, 20, 18-2, 07, with smaller initial imperfections, in contrary to the first boundary condition, do not have the highest buckling loads, and are much lower than the specimen with no cutout. In the specimens pl-150-100, 05-30-0-20-2 and pl-150-100-40, 6-0-20-2.04, where the initial imperfections are approximately similar, the latest has the higher buckling load and almost near to the value of the buckling load of the specimen without cutout. Similar behavior could observe with specimen pl-100.07-49.97-0-20.2-2.05 which has the highest buckling load almost identical to the specimen without cutout. Hence, it can be concluded that as the distance of the cutout from the middle of the plate increases the buckling load increases. This behavior could be seen clearly in the current boundary condition which the effect of imperfection is not significant. The smallest buckling load for this aspect ratio belongs to the specimen pl-150-100-4, 275-34, 425-20, 25-2, 07, because the cutout is located in the shortest distance from the middle of the plate.

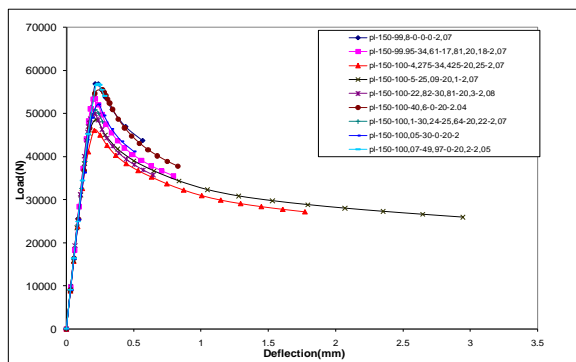


**Fig.24**  
Load-displacement curve for specimens with aspect ratio 1.5 and second boundary condition.

### 13 CONCLUSIONS

Buckling of rectangular plates with circular cutouts with a diameter of  $0.2b$  and a thickness ratio of  $b/t = 0.02$  was investigated under two boundary conditions: first, clamped boundary conditions for two loaded edges and free boundary conditions on the other edges (*CFCF*); second, clamped boundary conditions for two loaded edges and simply supported boundary conditions on the other edges with four aspect ratios using the finite element analysis and experimental tests. In specimens with circular cutouts, in addition to the aspect ratio, the effect of changing the location or area of the cutout on the buckling analysis was investigated. The experimental results closely resemble to the numerical analysis results for analysis of the buckling of rectangular plates, Conclusions of this study can be summarized as follows:

1. Comparison of the curves resulting from numerical and experimental analyses shows that these curves are closely compatible.
2. In most cases, the difference in the buckling loads calculated with numerical and experimental methods is less than 2%.
3. Furthermore, there is striking similarity between the deformations created by finite elements method and by

- experimental tests in the buckling and post-buckling states.
4. The buckling load in all specimens is lower than the yield load, and elastic buckling occurred in all specimens.
  5. The maximum effect of a cutout ( $d/b = 0.2$ ) is a 12% reduction in the buckling load compared to the specimen without cutouts.
  6. With increasing aspect ratio, the buckling load decreases considerably.
  7. The effective longitudinal distance from the middle of the plate is about 20% of the length of the plate. When the cutout lies outside this region it will have little effect on the buckling load of the plate.
  8. Due to free boundary conditions along the lateral edges of the specimens, changing the location of the cutout in the transverse direction has very little effect on the buckling load.
  9. The amount of initial imperfection has no effect of the post-buckling behavior of the rectangular plate.
  10. For the second boundary condition as the aspect ratio increases, the buckling load increases which is different from that observed for the first boundary condition. Hence, it can be concluded that the boundary condition could have a great influence of buckling behavior of the steel plates.
  11. For second boundary condition the effect of initial imperfection is not significant and as the distance of the cutout from the middle of the plate increases the buckling load increases.

## REFERENCES

- [1] Timoshenko S.P., Gere J.M., 1961, *Theory of Elastic Stability*, McGraw-Hill Book Company, New York.
- [2] El-Sawy Khaled M., Nazmy Aly S., 2001, Effect of aspect ratio on the elastic buckling of uniaxially loaded plates with eccentric holes, *Thin-Walled Structures* **39**: 983-998.
- [3] El-Sawy Khaled M., Nazmy Aly S., Ikbal Martini M., 2004, Elasto-plastic buckling of perforated plates under uniaxial compression, *Thin-Walled Structures* **42**: 1083-1101.
- [4] Narayanan R., Chow F.Y., 1984, Ultimate capacity of uniaxially compressed perforated plates, *Thin-Walled Structures* **2**: 241-264.
- [5] Shanmugam N.E., Thevendran V., Tan Y.H., 1999, Design formula for axially compressed perforated plates, *Thin-Walled Structures* **34**: 1-20.
- [6] Roberts T.M., Azizian Z.G., 1984, Strength of perforated plates subjected to in-plane loading, *Thin-Walled Structures* **2**: 153-164.
- [7] Mignot F., Puel J-P., Suquet P-M., 1980, Homogenization and bifurcation of perforated plates, *Engineering science* **18**: 409-414.
- [8] Yetterman A.L., Brown C.J., 1985, The elastic stability of square perforated plates, *Computer & Structures* **21**(6): 1267-1272.
- [9] Maan F.S., Querin O.M., Barton D.C., 2007, Extension of the fixed grid finite element method to eigenvalue problems, *Advances in Engineering Software* **38**(8-9): 607-617.
- [10] Singh Anand V., Tanveer M., 2006, Eigenvalue analysis of doubly connected plates with different configurations, *Journal of Sound and Vibration* **295**: 76-93.
- [11] Aydin Komur M., Sonmez M., 2008, Elastic buckling of rectangular plates under linearly varying in-plane normal load with a circular cutout, *Mechanics Research Communications* **35**(6): 361-371.
- [12] Rahai A.R., Alinia M.M., Kazemi S., 2008, Buckling analysis of stepped plates using modified buckling mode shapes, *Thin-Walled Structures* **46**: 484-493.
- [13] Eccher G., Rasmussen K.J.R., Zandonini R., 2008, Elastic buckling analysis of perforated thin-walled structures by the isoparametric spline finite strip method, *Thin-Walled Structures* **46**: 165-191.
- [14] Maiorana E., Pellegrino C., Modena C., 2009, Elastic stability of plates with circular and rectangular holes subjected to axial compression and bending moment, *Thin Walled Structure* **47**(3): 241-255.
- [15] Eccher G., Rasmussen K.J.R., Zandoninib R., 2009, Geometric nonlinear isoparametric spline finite strip analysis of perforated, *Thin-walled structures* **47**(2): 219-232.
- [16] Paik J.K., 2008, Ultimate strength of perforated steel plates under combined biaxial compression and edge shear loads, *Thin-Walled Structures* **46**: 207-213.